Electrophoretic Mobility, Zeta Potential, and Fixed Charge Density of Bovine Knee Chondrocytes, Methyl Methacrylate−Sulfopropyl Methacrylate, Polybutylcyanoacrylate, and Solid Lipid Nanoparticles

Yung-Chih Kuo* and Ta-Wei Lin

Department of Chemical Engineering, National Chung Cheng University, Chia-Yi, Taiwan 62102, Republic of China

Received: October 31, 2005; In Final Form: December 12, 2005

The electrophoretic mobility and zeta potential of bovine knee chondrocytes (BKCs), methyl methacrylate−sulfopropyl methacrylate (MMA−SPM) nanoparticles (NPs), polybutylcyanoacrylate (PBCA) NPs, and solid lipid nanoparticles (SLNs) were investigated under the influences of Na^+, K^+, and Ca^{2+} with various ionic strengths. The fixed charge density in the surface layers of the four biocolloidal particles was estimated from the experimental mobility of capillary electrophoresis with a theory of soft charged colloids. The results revealed that, for a specific cationic species, the absolute values of the electrophoretic mobility, the zeta potential, and the fixed charge density decreased with an increase in ionic strength. For a constant ionic strength, the effect of ionic species on the reduction in the absolute values of the electrophoretic mobility, the zeta potential, and the fixed charge density followed the order $Na^+ > K^+ > Ca^{2+}$ for the negatively charged BKCs, MMA−SPM NPs, and SLNs. The reverse order is true for the positively charged PBCA NPs.

1. Introduction

Electrophoretic behavior is one of the electrokinetic phenomena of colloidal particles under the affection of an external electric field. High performance capillary electrophoresis is an efficient analytic technique recently developed for the separation of charged entities via their electricity difference in electrolyte solution. For the investigation on the surface charge properties of mammalian cells, capillary electrophoresis (CE) was applied to examine the electrophoretic mobility of rat dorsal root ganglion neurons (RDRGNs) in a calcium-containing medium.[1] It was concluded that an increase in calcium content yielded a decrease in the absolute value of the RDRGNs' mobility. The electrophoretic mobility of human erythrocytes in various ionic strengths and pH values was studied by Kawahata et al.[2] It was generally observed that the absolute value of the mobility decreases with an increase in ionic strength, and the dissociations of the carboxyl groups of sialic acid in the surface layer of human erythrocytes were employed to explain the experimental results. Electrical characteristics of PC 12 neurons were analyzed by CE; however, the cells were regarded as rigid spheres.[3] It was drawn that the absolute value of the mobility and the zeta potential decrease with an increase in calcium concentration. Since the electric properties of ionogenic groups on the cellular surface could be adjusted by the surrounding electrolyte ions, CE was esteemed to be applicable to resolve the alteration in the traits of the surface groups.[4] For polymeric nanoparticles (NPs), the charged characteristics can also be evaluated by utilizing CE. An increase in the particulate diameter of polystyrene NPs led to a decrease in the absolute value of the electrophoretic mobility, and a high applied voltage and appropriate pH value were concluded to be favorable to the NP separation.[5,6] Furthermore, desorption of physically adsorbed orosomucoid from biocompatible polyisobutylcyanoacrylate was determined by CE.[7] The electrophoretic mobility and zeta potential of colloidal latexes could be modified by incorporating human serum albumin or immunoglobulin-G on the polymer surfaces.[8] For solid lipid nanoparticles (SLNs), reduction in the absolute value of the zeta potential was observed by the treatment of light and heat, rendering an increase in the particulate diameter.[9] Moreover, the surface charge properties would greatly influence the NP preservations,[10] the NP−animal cell interactions,[11] and the subsequent applications such as drug loading and entrapment.

In the early electrophoretic theories, Smoluchowski developed a model for rigid spherical colloids. Smoluchowski's formula, first revealing the relationship between the electrophoretic mobility, μ, and the zeta potential, ζ, is shown below.[12]

$$\mu = \frac{\epsilon_r \epsilon_0}{\eta}\zeta \tag{1}$$

where ϵ_r, ϵ_0, and η are, respectively, the relative permittivity, the permittivity of a vacuum, and the viscosity of the surrounding fluid. Note that eq 1 is valid for the case of $a \gg 1/\kappa$, where a and κ are, respectively, the particle radius and the reciprocal of the Debye screening length or the so-called double-layer thickness. Huckel extended the theory of hard spheres to the case of $a \ll 1/\kappa$ and derived a similar resultant formula, where a coefficient of 2/3 on the right-hand side of eq 1 emerges; that is, compared with a very thin double layer, μ is reduced by 2/3 for a very thick double layer. Ohshima and Ohki proposed a soft particle model by combining the theory of rigid spherical colloids with the theory of completely permeable polyelectrolytes.[13] The geometrical feature of a soft particle was regarded as a solid core covered with an ion-penetrable charged membrane. A softness parameter was introduced in the soft particle model for depicting the compressibility of the external polyelectrolyte layer.[14]

* To whom correspondence should be addressed. Phone: 886-5-272-0411 ext. 33459. Fax: 886-5-272-1206. E-mail: chmyck@ccu.edu.tw.

10.1021/jp056266f CCC: $33.50
Published on Web 01/12/2006

In the present study, the surface charge properties of bovine knee chondrocytes (BKCs), methyl methacrylate−sulfopropyl methacrylate (MMA−SPM) nanoparticles (NPs), polybutylcyanoacrylate (PBCA) NPs, and solid lipid nanoparticles (SLNs) were analyzed. The selected four particles represented the typical types of charged biocolloidal surfaces. Articular chondrocytes presented specific electrical properties, which were varied when inflammations or diseases occurred.[15] Moreover, charged characteristics of biodegradable NPs would influence not only the particulate flocculation during preservation but also the colloidal drug-releasing behavior and their interaction with biological cells. Hence, the electrophoretic mobility and the zeta potential of BKCs and the three synthetic biocompatible NPs were evaluated under various ionic strengths and ionic species. The fixed charge densities of the four biocolloids were estimated by the soft particle model with appropriate surface softness, which could be a directory parameter for particulate mutual interactions. Finally, the limit electrophoretic mobility and the limit fixed charge density of the four biocolloids were calculated.

2. Experimental and Theoretical Section

Preparation of BKCs. Isolation, counting, viability assessment, identification, cryopreservation, and cultivation of BKCs from calves were described in our previous study.[16] Concisely, the separation of BKCs from bovine knee cartilage combines the following procedures: (i) mechanical disaggregation, (ii) centrifugation, and (iii) enzymatic segmentation, where basement membranes in finely chopped tissue were dissected by 18% type II collagenase (Sigma) for the exposure of BKCs. 1.6×10^5 BKCs in 4 mL of Dulbecco's modified eagle's medium (DMEM, Sigma) were centrifuged at 420*g* and washed by tris(hydroxymethyl)aminomethane (Tris buffer, RDH, 99.5%). BKCs were centrifuged again and resuspended in 4 mL of Tris buffer with a specific ionic species and ionic strength; that is, the BKC density in the cellular suspension is about 4×10^4 cells/mL. Note that the typical medium for BKC cultivation is DMEM containing 1.113×10^{-1} M Na^+, 5.366×10^{-3} M K^+, and 1.802×10^{-3} M Ca^{2+}. The ionic level can, however, be diverse for a particular purpose of the mammalian cell cultures.

Preparation of MMA−SPM, PBCA, and SLNs. Fabrication of MMA−SPM NPs and PBCA NPs was reported previously.[10] Briefly, copolymerization of 4.5% methyl methacrylate (Fluka) and 0.5% sulfopropyl methacrylate (Aldrich) was initiated by 0.03% ammonim persulfate (Sigma). PBCA NPs were synthesized in the presence of 1% butylcyanoacrylate (Sicomet) in an acidic medium containing 1% dextran 70000 (Fluka). Polysorbate 80 (FisherScientific) was coated on the external surfaces of the NPs. The MMA−SPM and PBCA NPs were fairly monodisperse with cumulant *Z*-average diameters of 68.4 and 129.9 nm, respectively.

SLNs were prepared by the microemulsion method[18] with minor modifications. Briefly, 6% (w/w) tripalmitin (Fluka) and 1% (w/w) cacao butter (OCG Cacao Inc.) were melted at 70 °C, and 7% (w/w) L-A-phosphatidylcholine (Sigma), 4.5% (w/w) cholesteryl hemisuccinate (Sigma), 9.2% (w/w) 1-butanol (Riedel-de Haën), 2.4% (w/w) taurocholate (Sigma), and 69.9% (w/w) deionized water were mixed with the melted oil phase to form a microemulsion. A 1 mL portion of the microemulsion was added into 10 mL of 2 °C deionized water at 300 rpm for 15 min. After filtration by an 8 μm filter paper, 2% (w/v) D-trehalose (Sigma) was added into the filtrate, which was then freezed at 4 °C for 30 min, −20 °C for 30 min, and −80 °C for 2 h. SLNs were obtained by lyophilization (Eyela) at −80 °C for 24 h. The cumulant *Z*-average diameter of the present monodispersed SLNs was 264.6 nm.

An 8 mg portion of NPs was suspended in 4 mL of Tris buffer with a specific ionic species and ionic strength; that is, the NP density in the colloidal suspension is about 2 mg/mL.

Zeta Potential and Capillary Electrophoresis. The zeta potentials of the four biocolloids were measured by a zeta sizer 3000 HS_A with photo correlation spectroscopy (Malvern Instruments, version 1.41) under the following conditions: 25 °C, pH 7.2, and $\epsilon_r = 75.6$. The migration time of CE, *t*, was examined by P/ACE-2100 with Gold data acquisition software (Beckman Coulter) followed by a UV detector under the following conditions: 37 °C, pH 7.2, applied external voltage $V = 10$ kV, and wavelength of absorbance 214 nm. For the apparent geometry of the CE capillary, the total capillary length, *L*, the effective capillary length, *l*, and the inner diameter were, respectively, 43cm, 36.5 cm, and 75 μm. A fresh capillary was rinsed by 0.1 N HCl, 0.1 N NaOH, and deionized water for activation. To avoid electroosmosis, a coating of 5% poly(ethylene oxide) 600000 (Aldrich) on the capillary wall was required before filling the internal capillary lumen up with Tris buffer. Thus, the electrophoretic mobility can be determined experimentally by

$$\mu = \frac{u}{E} = \frac{l/t}{V/L} = \frac{lL}{Vt} \tag{2}$$

where *u* and *E* are, respectively, the particulate average velocity and the applied electric field.

Theory. The theoretical foundation invoked in the present study was the soft particle model, which assumes that a colloidal particle comprises an inner hard core and an external charged layer. These assumptions are appropriate to the description of the present biocolloids. The key formulations were shown below.[14]

$$\mu = \frac{\epsilon_r \epsilon_0}{\eta} \frac{\psi(0)/\kappa_m + \psi_{DON}/\lambda}{1/\kappa_m + 1/\lambda} f\left(\frac{d}{a}\right) + \frac{zeN}{\eta\lambda^2} \tag{3}$$

$$\psi_{DON} = \frac{kT}{ve} \ln\left[\frac{zN}{2\upsilon n} + \left\{\left(\frac{zN}{2\upsilon n}\right)^2 + 1\right\}^{1/2}\right] \tag{4}$$

$$\psi(0) = \frac{kT}{ve}\left(\ln\left[\frac{zN}{2\upsilon n} + \left\{\left(\frac{zN}{2\upsilon n}\right)^2 + 1\right\}^{1/2}\right] + \frac{2\upsilon n}{zN}\left[1 - \left\{\left(\frac{zN}{2\upsilon n}\right)^2 + 1\right\}^{1/2}\right]\right) \tag{5}$$

$$\kappa_m = \kappa\left[1 + \left(\frac{zN}{2\upsilon n}\right)^2\right]^{1/4} \tag{6}$$

$$\kappa = \left(\frac{2Ie^2\upsilon^2 N_A}{\epsilon_r \epsilon_0 kT}\right)^{1/2} \tag{7}$$

$$f\left(\frac{d}{a}\right) = \frac{2}{3}\left[1 + \frac{1}{2(1 + d/a)^3}\right] \tag{8}$$

$$\mu_\infty = \frac{zeN_\infty}{\eta\lambda^2} \tag{9}$$

where η, $\psi(0)$, ψ_{DON}, κ_m, $1/\lambda$, *d*, *z*, *e*, *N*, *k*, *T*, υ, *n*, *I*, N_A, μ_∞, and N_∞ are, respectively, the fluidic viscosity, the potential on the solution−particle interface, the Donnan potential, the Debye screening length for the particle surface layer, the surface softness, the ion-penetrable thickness, the valence of fixed groups in the surface layer, the elementary charge, the fixed charge density in the surface layer, the Boltzmann constant, the absolute temperature, the valence of counterions, the bulk

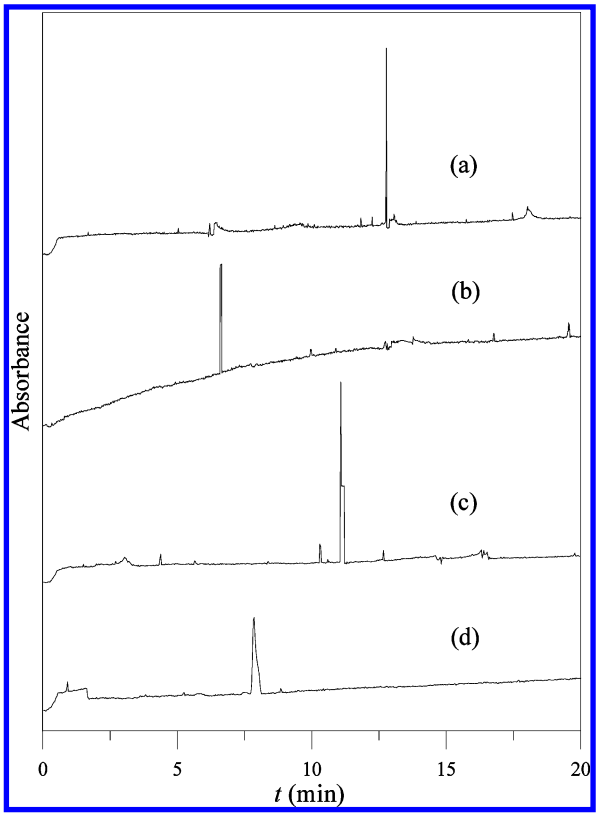

Figure 1. Typical signals of BKCs, MMA−SPM NPs, PBCA NPs, and SLNs from an UV detector connected to a CE system: (a) BKCs; (b) MMA−SPM NPs; (c) PBCA NPs; (d) SLNs.

TABLE 1: Electrophoretic Mobility and Zeta Potential of the Four Biocolloids in the Original Tris Buffer

	ζ (mV)	μ ($\times 10^{-8}$ m^2 s^{-1} V^{-1})	μ_S ($\times 10^{-8}$ m^2 s^{-1} V^{-1})	D (%)
BKCs	−23.2	−2.130	−2.237	5.02
MMA−SPM	−62.3	−5.375	−6.032	12.22
PBCA	30.1	2.736	2.914	6.51
SLN	−34.6	−3.501	−3.350	4.31

concentration of counterions, the ionic strength of the electrolyte solution, the Avogadro number, the limit electrophoretic mobility, and the limit fixed charge density in the surface layer. A larger d/a value represented a softer particle. For polyelectrolytes, the d/a value approaches infinity. On the basis of the mobility data obtained from CE experiments with the most appropriately fitted $1/\lambda$, the N value can be evaluated by solving eqs 3−8 subject to the conditions $\epsilon_r = 75.6$, $T = 37$ °C, $\eta = 0.691$ cp, and $z = 1$. Thus, employment of the soft particle model is beneficial for achieving the relevant electrical and geometrical parameters, which become unreachable owing to sophistication in some advanced models. When n increases, $\psi(0)$ and ψ_{DON} reduce and κ_m increases. Hence, μ_∞ and N_∞ of the four biocolloids can be estimated by eq 9 for an extremely large n value.

The deviation, D, between the electrophoretic mobility measured by CE through eq 2 and that converted by the zeta potential through eq 1 (the Smoluchowski mobility), μ_S, is defined below.

$$D = \left|\frac{\mu - \mu_S}{\mu}\right| \qquad (10)$$

3. Results and Discussion

Figure 1 shows the typical UV absorbance of BKCs, MMA−SPM NPs, PBCA NPs, and SLNs in the original Tris buffer with an ionic strength of about 4×10^{-6} M. Through eq 2, μ could be evaluated by t exhibited in this figure. μ and the corresponding ζ were listed in Table 1. As revealed in this table, the larger $|\zeta|$, the higher $|\mu|$. For the four examined biocolloids, the magnitude of $|\mu|$ and $|\zeta|$ followed the order BKCs < PBCA NPs < SLNs < MMA−SPM NPs. The charged groups of articular chondrocytes were COO^- and SO_3^- on chondroitin sulfate (CS) and SO_3^- on keratin sulfate (KS),[19] where CS and KS comprised proteoglycans (PGs) on the cellular surface[20] and the amount of CS was larger than that of KS.[21] In addition, the types of PGs in the cartilage of the patients with osteoarthritis or rheumatoid arthritis were more than those in normal articular tissue. In pathologically changed chondrocytes, structurally destroyed CS and KS caused a reduced charge density and a decreased cationic absorption, rendering a lower ability to form PG aggregates on the cellular surfaces.[22] The surface charge group on MMA−SPM NPs was SO_3^- of SPM.[23] The reason for positively charged PBCA NPs was the adsorption of H^+ on CN groups of butylcyanoacrylate monomer from the acidic medium when emulsion polymerization took place.[24] For SLNs, the external lipid bilayer containing phosphatidylcholine was about 5−6 nm,[25,26] and the charged group on SLNs was SO_3^- of taurocholate, which distributed over the outer bilayer surface.[27]

Parts a−c of Figure 2 showed, respectively, the zeta potential, the electrophoretic mobility, and the fixed charge density of BKCs for various ionic species and ionic strengths. Here, $1/\lambda = 3.0$ nm was the best fitted parameter for BKCs. $1/\lambda$ was about 2.5−3.0 nm for human erythrocytes and human umbilical vein endothelial cells.[2,17] As exhibited in Figure 2b, the theoretical curves connecting CE data were calculated by the soft particle model. As revealed in parts a−c of Figure 2, respectively, $|\zeta|$, $|\mu|$, and $|N|$ decreased as I increased for a fixed ionic species. For a constant I, the low-to-high sequence of $|\zeta|$, $|\mu|$, and $|N|$ for the three cationic species abided by the following order: $Na^+ > K^+ > Ca^{2+}$, as presented in Figure 2b. Since the molarity of Ca^{2+} was less than that of Na^+ or K^+ for a constant I, the influence on the reduction in $|\zeta|$, $|\mu|$, and $|N|$ of BKCs for monovalent cations was stronger than that for divalent cations. Besides, $|\zeta|$, $|\mu|$, and $|N|$ of K^+ were larger than those of Na^+ for a fixed I. This result was consistent with the theoretical prediction for electrolyte solutions with a constant I and a fixed counterionic valence but different ionic sizes.[28] Since the ionic radius of Na^+ was smaller than that of K^+, the rationale behind this result was that cations with a smaller volume would generate a greater penetrating ability into the outer surface layer of biocolloids and cause a stronger shielding effect on the negative electricity. As revealed in Figure 2b, μ_S converted from the results of Figure 2a agreed qualitatively with the trend of μ when I increased. The average deviation evaluated by eq 10 was about 14%, demonstrating that the hard sphere theory was not a very reasonable description for the electrophoresis of BKCs. The estimated μ_∞ and N_∞ values of BKCs were -3.9×10^{-3} M and -4.92×10^{-9} m^2 s^{-1} V^{-1}, respectively. Comparing parts a−c of Figure 2, it could be drawn that the larger $|N|$, the higher $|\zeta|$ and $|\mu|$.

Variations in ζ, μ, and N of MMA−SPM NPs as a function of ionic strength were shown, respectively, in parts a−c of Figure 3. For MMA−SPM NPs, the best fitted $1/\lambda$ was 1.8 nm. As presented in these figures, $|\zeta|$, $|\mu|$, and $|N|$ decreased as I increased for a specific electrolyte species. Since the freshly

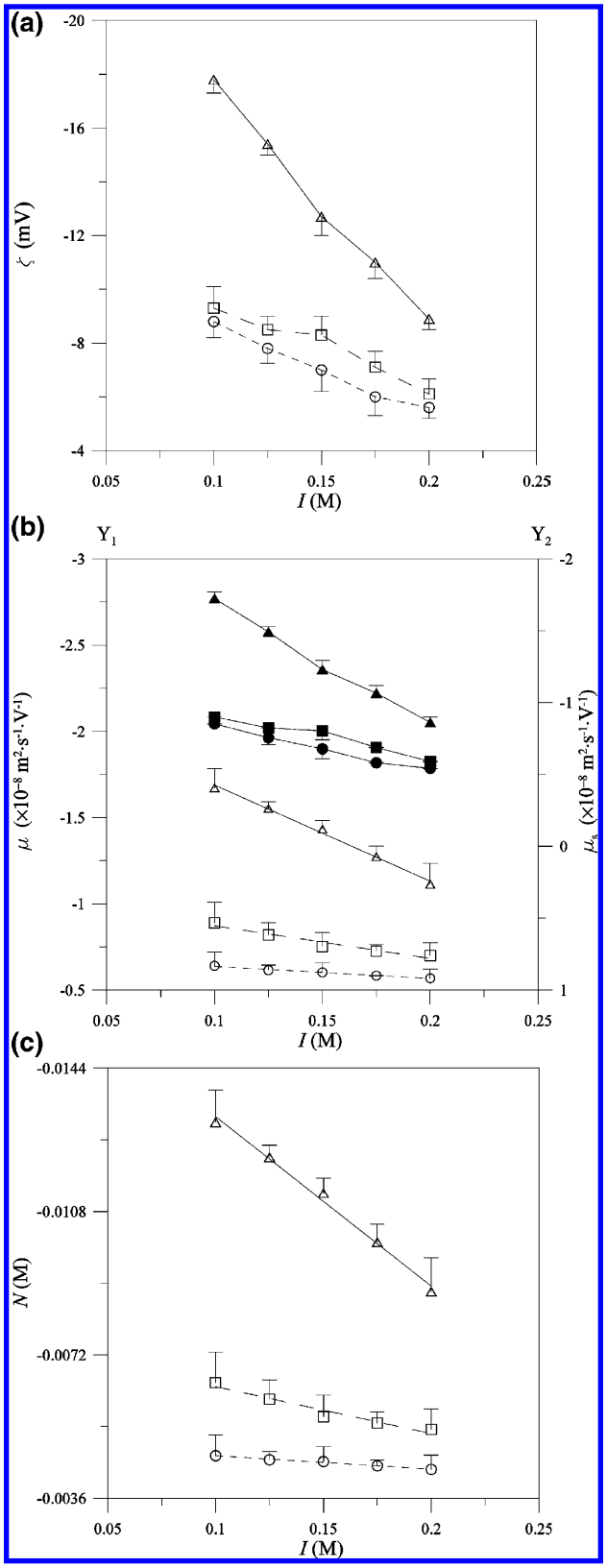

Figure 2. (a) Variation in the zeta potential of BKCs as a function of ionic strength: (○) Na^+; (□) K^+; (△) Ca^{2+}. (b) Variation in the electrophoretic mobility of BKCs as a function of ionic strength. Experimental data (Y_1 axis employed): (○) Na^+; (□) K^+; (△) Ca^{2+}. Theoretical results evaluated by the soft particle model (Y_1 axis employed): (- - -) Na^+; (— — —) K^+; (—) Ca^{2+}. Theoretical data estimated by the Smoluchowski formula (data connected by a solid line and Y_2 axis employed): (●) Na^+; (■) K^+; (▲) Ca^{2+}. (c) Variation in the fixed charge density of BKCs as a function of ionic strength: (○) Na^+; (□) K^+; (△) Ca^{2+}.

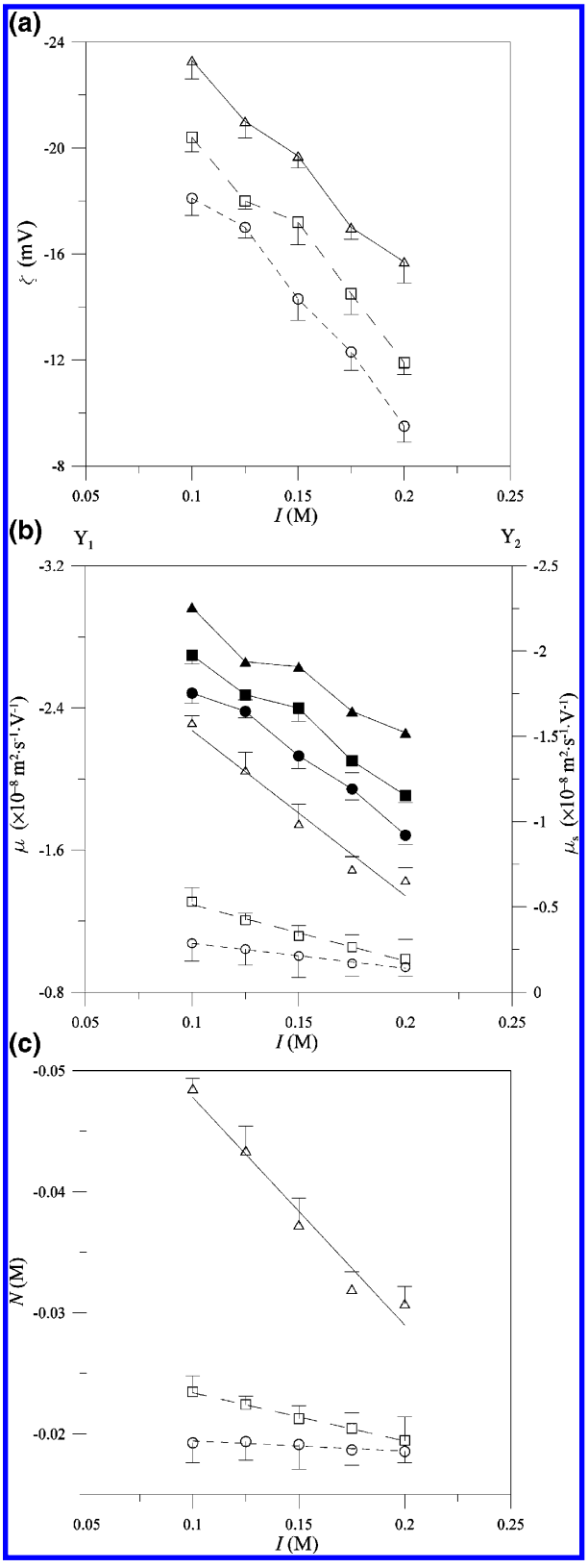

Figure 3. (a) Variation in the zeta potential of MMA−SPM NPs as a function of ionic strength: (○) Na^+; (□) K^+; (△) Ca^{2+}. (b) Variation in the electrophoretic mobility of MMA−SPM NPs as a function of ionic strength. Experimental data (Y_1 axis employed): (○) Na^+; (□) K^+; (△) Ca^{2+}. Theoretical results evaluated by the soft particle model (Y_1 axis employed): (- - -) Na^+; (— — —) K^+; (—) Ca^{2+}. Theoretical data estimated by the Smoluchowski formula (data connected by a solid line and Y_2 axis employed): (●) Na^+; (■) K^+; (▲) Ca^{2+}. (c) Variation in the fixed charge density of MMA−SPM NPs as a function of ionic strength: (○) Na^+; (□) K^+; (△) Ca^{2+}.

prepared MMA−SPM NPs were highly charged, and the decreases in $|\zeta|$ and $|\mu|$ by the addition of Na^+, K^+, and Ca^{2+} to MMA−SPM NP suspensions were relatively evident, SO_3^- on MMA−SPM NPs was sensitive to the surrounding cations. As compared with the MMA−SPM NP data given in Table 1, the order of magnitude of the reduction in $|\zeta|$ and $|\mu|$ by the counterionic additions followed $Na^+ > K^+ > Ca^{2+}$ for a constant I. Figure 3b also showed the results of μ_S converted from ζ. As displayed in this figure, $\mu_S(I)$ was qualitatively consistent with $\mu(I)$. The average D value was about 25%, suggesting that the Smoluchowski's formula was not appropriate for the application to MMA−SPM NPs. The apparent disagreement arose mainly from the low potential assumption made in Smoluchowski's theory. The evaluated μ_∞ and N_∞ values of MMA−SPM NPs were -1.3×10^{-2} M and -5.89×10^{-9} m^2 s^{-1} V^{-1}, respectively. That a larger $|N|$ would cause higher $|\zeta|$ and $|\mu|$ can also be concluded from Figure 3.

Parts a−c of Figure 4 presented, respectively, the variations in ζ, μ, and N of PBCA NPs as a function of I. The best fitted $1/\lambda$ was 1.9 nm for PBCA NPs. As exhibited in these figures, ζ, μ, and N reduced as I increased for a fixed cationic species. Since PBCA NPs were positively charged with the potential determining ions H^+, the governing indifferent counterions were Cl^-. The influence on the reduction in ζ, μ, and N by the addition of Ca^{2+} was greater than that of Na^+ and K^+ because the molarity of Cl^- in $CaCl_2$ solution was larger than that in NaCl or KCl solution for a constant I. Furthermore, for a constant I, ζ, μ, and N of K^+ was lower than those of Na^+. This was because the ionic radius of K^+ was larger than that of Na^+, rendering a lower exclusive volume and a more approachable behavior of Na^+ near PBCA NP surfaces, and a higher electrostatic potential of the positively charged particles for the Na^+-relating system.[29,30] Hence, for a fixed I, the order of importance of added cationic species to the influence on the decrease in the surface charge properties was $Ca^{2+} > K^+ > Na^+$, as compared with the data of PBCA NPs in Table 1. As I increased, the qualitative tendency to the reduction in μ_S was in agreement with that in μ. The average D value of PBCA NPs was about 10%, which was much lower than that of MMA−SPM NPs. This was because the ζ of PBCA NPs was much lower than the ζ of MMA−SPM NPs, leading to a more accurate Smoluchowski prediction for the former. The calculated μ_∞ and N_∞ values of PBCA NPs were 9.7×10^{-3} M and 4.88×10^{-9} m^2 s^{-1} V^{-1}, respectively. It could also be concluded from Figure 4 that higher ζ and μ corresponded to a larger N.

Variations in ζ, μ, and N of SLNs as a function of I were presented, respectively, in parts a−c of Figure 5. The best fitted $1/\lambda$ was 1.7 nm for SLNs. As presented in these figures, the larger I, the lower $|\zeta|$, $|\mu|$, and $|N|$ for a specific ionic species. As compared with the SLN results specified in Table 1, the effect of electrolyte addition on the reduction in $|\zeta|$ and $|\mu|$ followed the order $Na^+ > K^+ > Ca^{2+}$ for a constant I. Since the charged lipid bilayers of biomimic SLNs could be comparable to the membranes of BKCs, the electrical behavior of SLNs was similar to that of BKCs, except that the charge loading on SLN lipid surfaces was higher than that on BKC membrane layers. The converted μ_S was in extraordinarily good conformity with μ, where the average D value was about 5%, although assuming hard spherical SLNs was not definitely proper by intuition. The μ_∞ and N_∞ values of SLNs were, respectively, -1.2×10^{-2} M and -4.89×10^{-9} m^2 s^{-1} V^{-1}. A larger $|N|$ would lead to higher $|\zeta|$ and $|\mu|$, as expected in Figure 5.

For the four investigated biocolloids, a higher level of I not only compressed the thickness of the electrical double layer but

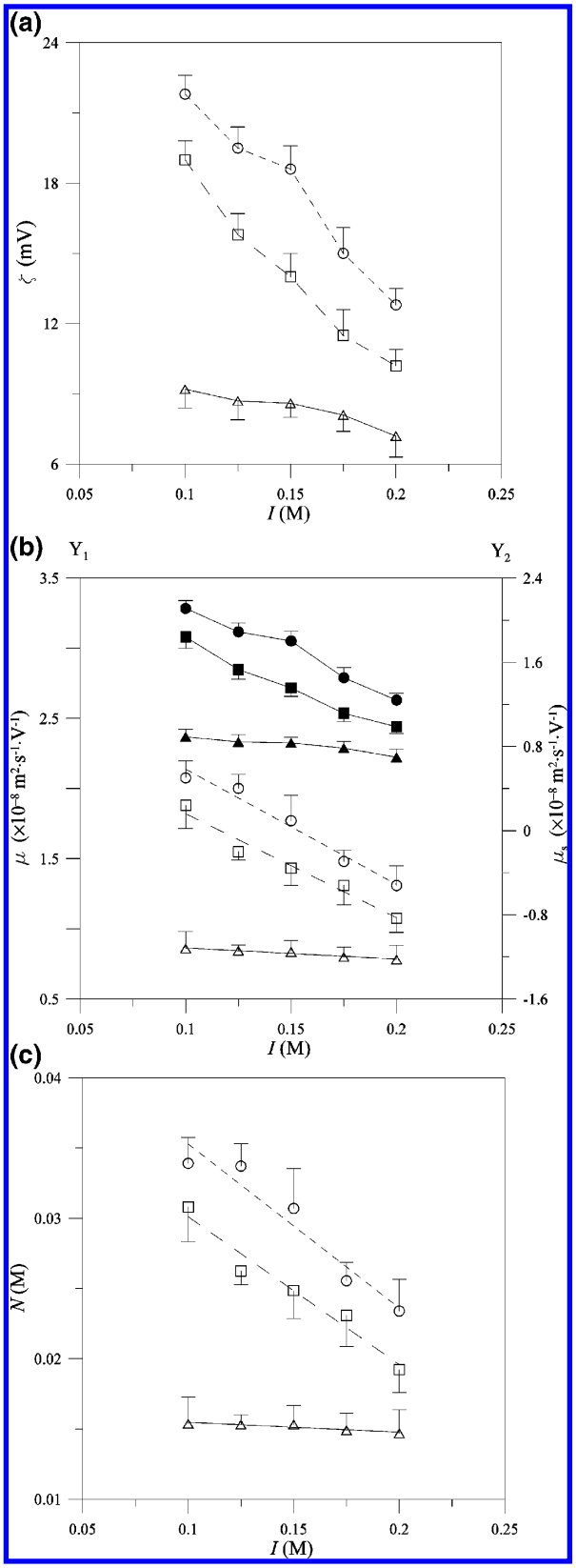

Figure 4. (a) Variation in the zeta potential of PBCA NPs as a function of ionic strength: (○) Na^+; (□) K^+; (△) Ca^{2+}. (b) Variation in the electrophoretic mobility of PBCA NPs as a function of ionic strength. Experimental data (Y_1 axis employed): (○) Na^+; (□) K^+; (△) Ca^{2+}. Theoretical results evaluated by the soft particle model (Y_1 axis employed): (- - -) Na^+; (— — —) K^+; (—) Ca^{2+}. Theoretical data estimated by the Smoluchowski formula (data connected by a solid line and Y_2 axis employed): (●) Na^+; (■) K^+; (▲) Ca^{2+}. (c) Variation in the fixed charge density of PBCA NPs as a function of ionic strength: (○) Na^+; (□) K^+; (△) Ca^{2+}.

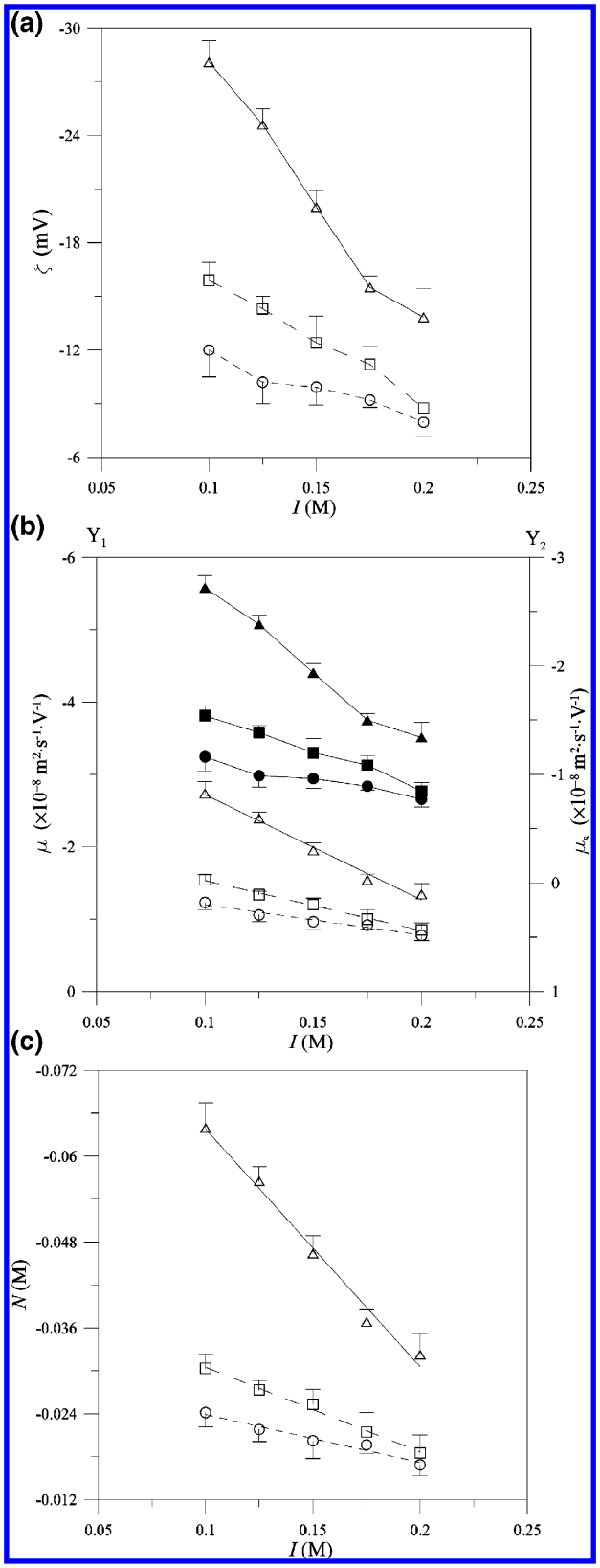

Figure 5. (a) Variation in the zeta potential of SLNs as a function of ionic strength: (○) Na^+; (□) K^+; (△) Ca^{2+}. (b) Variation in the electrophoretic mobility of SLNs as a function of ionic strength. Experimental data (Y_1 axis employed): (○) Na^+; (□) K^+; (△) Ca^{2+}. Theoretical results evaluated by the soft particle model (Y_1 axis employed): (- - -) Na^+; (— — —) K^+; (—) Ca^{2+}. Theoretical data estimated by the Smoluchowski formula (data connected by a solid line and Y_2 axis employed): (●) Na^+; (■) K^+; (▲) Ca^{2+}. (c) Variation in the fixed charge density of SLNs as a function of ionic strength: (○) Na^+; (□) K^+; (△) Ca^{2+}.

also neutralized the charged groups in the particulate surface layer. Hence, a lower $|\mu|$ resulted from a higher I in the present study. Also, the order of magnitude of $|N_\infty|$ followed BKCs < PBCA NPs < SLNs < MMA−SPM NPs. This order was the same as the order of the surface charge properties listed in Table 1 for Tris buffer without further addition of electrolytes. Although SO_3^- on MMA−SPM NPs was very responsive to cations, the electroneutralization effect was still incomplete at high electrolyte concentration. Also, the magnitude of $|\mu_\infty|$ became commensurate for PBCA NPs, SLNs, and BKCs. Comparison of $|N_\infty|$ and $|\mu_\infty|$ of the three artificial biocolloids showed that $|\mu_\infty|$ of BKCs was noticeably high because BKCs possessed a relatively large surface softness. The surface charge properties of mammalian cells would also affect a wide range of their applications including cellular adhesion[31] and aggregation.[32] When rat basophilic leukemia cells attached to solid surfaces, N and $1/\lambda$ would vary from −0.016 to −0.025 M and from 2.0 to 2.3 nm, respectively.[33] Moreover, N could be altered by biochemical reactions on the external membrane layer or by metabolisms in the internal cellular cytoplasm.[1] Articular chondrocytes are required to maintain a low Na^+/K^+ ratio via the regulation of the Na^+, K^+-ATPase. An addition of extracellular Na^+ could induce a higher activity of the Na^+, K^+-ATPase, rendering ionic transport and N variation in articular chondrocytes.[34,35] Besides, colloidal polymeric particles with a large $|N|$ would highly disperse in a suspension; on the contrary, a small $|N|$ and a small $1/\lambda$ would cause particulate aggregation.[36] In a vaccine delivery system, N could be modified by incorporating charged polyamino acids or proteins with NP carriers, yielding an enhanced interaction between carriers and human dendritic cells.[37,38]

4. Conclusions

In summary, the surface charge properties of BKCs, MMA−SPM NPs, PBCA NPs, and SLNs were studied for the three most physiologically encountered cations, Na^+, K^+, and Ca^{2+}, under various ionic strengths. BKCs possessed the highest surface softness among the four typical biocolloidal surfaces, rendering a promoted limit μ value at the comparatively low limit N value. On the basis of a soft particle model, the experimental electrophoretic mobility, μ, was fitted by appropriate softness parameters and the fixed charge density, N, was calculated. For comparison, the theoretical μ_S, converted by the experimental zeta potential, ζ, was evaluated through Smoluchowski's formula, which could be applied to the present biocolloids for qualitative estimations. The smallest and largest average deviations between μ and μ_S of the four particles were, respectively, SLNs (∼5%) and MMA−SPM NPs (∼25%). The large deviation of the latter resulted from their highly charged nature. $|\zeta|$, $|\mu|$, and $|N|$ decreased as the ionic strength increased for a specific electrolyte solution. For the negatively charged BKCs, MMA−SPM NPs, and SLNs at a fixed ionic strength, Ca^{2+} held the weakest effect on the influence of ζ, μ, and N among the three cations, and Na^+, which had a smaller ionic radius, also produced a stronger effect on the influence of ζ, μ, and N than K^+. For the positively charged PBCA NPs, the reverse is true. The qualitative trend of the limit N value for the four investigated biocolloids was consistent with the surface charge properties in the original buffer without the addition of electrolytes.

Acknowledgment. This work is supported by the National Science Council of the Republic of China.

References and Notes

(1) Mironov, S. L.; Dolgaya, E. V. *J. Membr. Biol.* **1985**, *86*, 197.

(2) Kawahata, S.; Ohshima, H.; Muramatsu, N.; Kondo, T. *J. Colloid Interface Sci.* **1990**, *138*, 182.
(3) Young, T. H.; Hung, C. H.; Huang, S. W.; Hsieh, T. S.; Hsu, J. P. *J. Colloid Interface Sci.* **2005**, *285*, 557.
(4) van der Mei, H. C.; van de Belt-Gritter, B.; Doyle, R. J.; Busscher, H. J. *J. Colloid Interface Sci*. **2001**, *241*, 327.
(5) Radko, S. P.; Chrambach, A. *J. Chromatogr., B* **1999**, *722*, 1.
(6) VanOrman, B. B.; McIntire, G. L. *J. Microcolumn Sep*. **1989**, *1*, 289.
(7) Olivier, J. C.; Vauthier, C.; Taverna, M.; Puisieux, F.; Ferrier, D.; Couvreur, P. *J. Controlled Release* **1996**, *40*, 157.
(8) Nakamura, M.; Ohshima, H.; Kondo, T. *J. Colloid Interface Sci*. **1992**, *149*, 241.
(9) Freitas, C.; Muller, R. H. *Int. J. Pharm.* **1998**, *168*, 221.
(10) Kuo, Y. C. *Int. J. Pharm.* **2005**, *290*, 161.
(11) Kuo, Y. C.; Chung, C. Y. *J. Chin. Inst. Chem. Eng.* **2005**, *36*, 627.
(12) Hunter, R. J. *Foundations of Colloid Science*; Oxford University Press: Oxford, U.K., 1989; Vol. 1.
(13) Ohshima, H.; Ohki, S. *Biophys. J.* **1985**, *47*, 673.
(14) Ohshima, H. *J. Colloid Interface Sci*. **1994**, *163*, 474.
(15) Knudson, C. B.; Knudson, W. *Semin. Cell Dev. Biol*. **2001**, *12*, 69.
(16) Kuo, Y. C.; Chung, C. Y. *Biotechnol. Prog.* **2005**, *21*, 1708.
(17) Makiko, K.; Fukai, F.; Hirata, S.; Ohshima, H. *Colloids Surf., B* **1996**, *7*, 235.
(18) Cavalli, R.; Caputo, O.; Gasco, M. R. *Eur. J. Pharm. Sci.* **2000**, *10*, 305.
(19) Van Damme, M. P. I.; Tiglias, J.; Nemat, N.; Preston, B. N. *Anal. Biochem*. **1994**, *223*, 62.
(20) Mobasheri, A.; Carter, S. D.; Martin-Vasallo, P.; Sharkibaei, M. *Cell Biol. Int.* **2002**, *26*, 1.
(21) Mow, V. C.; Wang, C. C.; Hung, C. T. *OsteoArthritis Cartilage* **1999**, *7*, 41.
(22) Knudson, C. B.; Knudson, W. *Semin. Cell Dev. Biol*. **2001**, *12*, 69.
(23) Langer, K.; Marburger, C.; Berthold, A.; Kreuter, J.; Stieneker, F. *Int. J. Pharm*. **1996**, *137*, 67.
(24) Pirker, S.; Kruse, J.; Noe, Ch.; Langer, K.; Zimmer, A.; Kreuter, J. *Int. J. Pharm*. **1996**, *128*, 189.
(25) Nagle, J. F.; Tristram-Nagle, S. *Curr. Opin. Struct. Biol*. **2000**, *10*, 474.
(26) Risbo, J.; Jorgensen, K.; Sperotto, M. M.; Mouritsen, O. G. *Biochim. Biophys. Acta* **1997**, *1329*, 85.
(27) Travis, A. J. F.; Foster, L. H.; Robins, M. M. *Biophys. Chem.* **1995**, *54*, 253.
(28) Kuo, Y. C. *J. Phys. Chem. B* **2005**, *109*, 11727.
(29) Kuo, Y. C. *J. Chem. Phys.* **2003**, *118*, 398.
(30) Kuo, Y. C. *J. Chem. Phys.* **2003**, *118*, 8023.
(31) Kuo, Y. C. *J. Colloid Interface Sci.* **2005**, *288*, 36.
(32) Kuo, Y. C. *Colloids Surf., B*, in press.
(33) Makino, K.; Fukai, F.; Kawaguchi, T.; Ohshima, H. *Colloids Surf., B* **1995**, *5*, 221.
(34) Mobasheri, A.; Hall, A. C.; Urban, J. P. G.; France, S. J.; Smith, A. L. *Int. J. Biochem. Cell Biol.* **1997**, *29*, 649.
(35) Mobasheri, A.; Errington, R. J.; Golding, S.; Hall, A. C.; Urban, J. P. G. *Cell Biol. Int.* **1997**, *21*, 201.
(36) Makino, K.; Kado, H.; Ohshima, H. *Colloids Surf., B* **2001**, *20*, 247.
(37) Foged, C.; Brodin, B.; Frokjaer, S.; Sundblad, A. *Int. J. Pharm.* **2005**, *298*, 315.
(38) Jung, T.; Kamm, W.; Breitenbach, A.; Kaiserling, E.; Xiao, J. X.; Kissel, T. *Eur. J. Pharm. Biopharm.* **2000** *50*, 147.